

1
2
3
4
5
6
7
8
9
10
11
12
13
14
15
16
17
18
19
20
21
22
23
24
25

*Drug Screening using Shape-based Virtual Screening and In Vitro
Experimental Models of Cutaneous Leishmaniasis*

C. C. Santos¹; M. M. Batista¹, Asma Inam Ullah², Tummala Rama Krishna Reddy²
and Maria de Nazaré C. Soeiro^{1*}

¹Laboratory of Cellular Biology (LBC), Oswaldo Cruz Institute (IOC/FIOCRUZ),
CEP21040-360 Rio de Janeiro, RJ, Brasil.

² The Medicines Research Group, School of Health, Sport and Bioscience, College
of Applied Health and Communities, University of East London, Stratford campus,
Water Lane, UK.

*Corresponding author. Tel: +55-21-25621368; e-mail: soeiro@ioc.fiocruz.br

RUNNING TITLE: Leishmanicidal activity of Oxazolo[4,5-b] pyridine derivative
and benzimidazole derivative.

26

27 **Synopsis**

28 Cutaneous leishmaniasis (CL) is one of the most disregarded tropical neglected
29 disease with the occurrence of self-limiting ulcers and triggering mucosal damage and
30 stigmatizing scars, leading to huge public health problems and social negative
31 impacts. Pentavalent antimonials are the first-line drug for CL treatment for over 70
32 years and present several drawbacks in terms of safety and efficacy. Thus, there is an
33 urgent need to search for non-invasive, non-toxic, and potent drug candidates for CL.
34 In this sense, we have implemented a shape-based virtual screening approach and
35 identified a set of 32 hit compounds. *In vitro* phenotypic screenings were conducted
36 using these hit compounds to check their potential leishmanicidal effect towards
37 *Leishmania amazonensis*. The findings showed that two (Cp1 and Cp2) out of the 32
38 compounds revealed promising antiparasitic activities, exhibiting considerable
39 potency against intracellular amastigotes present in peritoneal macrophages (IC₅₀
40 values of 9.35 and 7.25 μM, respectively). Also, a sterile cidal profile was reached
41 at 20 μM after 48 hours of incubation, besides a reasonable selectivity (≈8), quite
42 similarly to pentamidine, an aromatic diamidine still in use clinically for
43 leishmaniasis. Cp1 with an Oxazolo[4,5-b]pyridine scaffold and Cp2 with a
44 benzimidazole scaffold could be developed further by lead optimization studies to
45 enhance their leishmanicidal potency.

46

47

48 **KEY WORDS:** Cutaneous leishmaniasis, *Leishmania amazonensis*, shape-based
49 virtual screening, *in vitro* experimental chemotherapy.

50

51 **Introduction**

52 Cutaneous leishmaniasis (CL) is a vector-borne tropical neglected disease caused by
53 over 20 different species of kinetoplastid parasites of the genus *Leishmania*. This
54 disfiguring and stigmatizing disease occurs through the injection of promastigote
55 forms into the mammals by infected female sandflies, triggering ulcers and
56 permanent scars at skin and/or oral and nasal mucosa injuries, thus contributing to
57 high social stigmatization and public health issue (WHO, 2020). Although about
58 1,2 million of new cases occur annually, CL does not have adequate treatment that
59 are mostly based on old and highly toxic drugs besides the occurrence of high number
60 of parasite species with drug resistance profile (Bailey *et al.*, 2019, Alvar *et al.*, 2012,
61 de Vries *et al.*, 2015, Van Bocxlaer *et al.*, 2019).

62 First line treatments include the clinical use of pentavalent antimonials drugs
63 developed 70 years ago that present several drawbacks in terms of efficacy, safety and
64 require long painful periods of administration (Eiras *et al.*, 2015, DNDi 2018). In the
65 case of antimonial resistance, the second-choice therapy includes pentamidine and
66 amphotericin B (deoxycholate), which also share the previous reported concerns and
67 limitations (Croft 2006, de Vries *et al.*, 2015). Up to now, the only oral and less toxic
68 alternative drug – Milteforan – is unavailable in many developing poorest countries
69 (Bilgic Temel 2019). Besides, the safer liposomal formulation of amphotericin B is
70 highly costly and still under evaluation for effectiveness against CL (Shirzadi 2019).
71 Last clinical trials for CL were mostly based on drug repurposing and/or combination
72 but unfortunately the overall findings were not very successful to demonstrate an
73 improvement of therapeutic efficacy, such as the combination of Pentavalent
74 antimonial with imiquimoid (Miranda-Verastequi *et al.*, 2009) and the topical use of
75 3% amphotericin B (Lopez *et al.*, 2018). A phase II clinical trial regarding a shorter
76 course of oral miltefosine administrated in combination with thermotherapy,

77 conducted in Peru and Colombia, ended in 2019 but the outcomes were not published
78 yet (Valencia *et al.*, 2013, [https://www.dndi.org/diseases-projects/portfolio/new-cl-](https://www.dndi.org/diseases-projects/portfolio/new-cl-combos)
79 [combos](https://www.dndi.org/diseases-projects/portfolio/new-cl-combos)).

80 Computer aided drug design is an efficient strategy to identify active compounds.
81 Shape-based screening has been successfully employed for the development of anti-
82 fungal and anti-bacterial agents (Swinney & Anthony, 2011). To employ this
83 approach, 3D structure of the target protein/receptor is not required. However, an
84 established active compound (defined as a query compound) against a target is a
85 starting point for this approach. The purpose of the shape-based screening is to
86 identify chemically diverse compounds that show similar biological activity as the
87 query compound. This is based on the principle that diverse structures that share
88 similar shape and electrostatic potential surface, or topology will have highest
89 probability to bind to the same pocket and consequently share the similar activity
90 (Kumar & Zhang, 2018). Due to the limited information on target proteins of
91 *Leishmania amazonensis* and the non-availability of quality 3D structures of target
92 proteins, we have carried out ligand-based shape screening approach using an
93 established active compound GNF5343 that is reported to display broad spectral anti-
94 parasitic activity (Khare *et al.*, 2016). We have identified a set of 32 hit compounds
95 from this study. Thus, the urgent need for safer and selective potent drugs associated
96 with promising aspects of identified diverse hit compounds encouraged us to perform
97 *in vitro* phenotypic screening-of these compounds upon amastigotes of *Leishmania*
98 *amazonensis*, which is one of the main agents of CL in the Americas (Martins 2014,
99 de Vries *et al.*, 2015).

100

101

102 **Methods**

103 *Compounds:* All 32 identified hit compounds (Chart 1 and Figure 1) that were
104 purchased from Asinex commercial vendor and the reference drug, Pentamidine (Pt),
105 were dissolved in DMSO (stock solutions at 20 mM) and fresh dilutions prepared
106 extemporaneously, with the final concentration never exceeding 0.6% for *in vitro*
107 experiments, which does not induce host cell toxicity (Santos *et al.*, 2019).

108 *Parasite strain and mammalian host cell cultures:* *Leishmania amazonensis* (strain
109 *LTB0016*) was used throughout the study. Male BALB/c mice were infected (10^6
110 amastigotes/20 μ L culture medium, via subcutaneous) at their foot paws, using a BD
111 ultrafine™ 6 mm syringe (15/64”) x 31 G, following previous reported protocol, with
112 minor modifications (Van Bocklaer *et al.*, 2019). After 30 days post infection, the
113 animal skin lesions were aseptically removed, and the parasites obtained by mechanic
114 dissociation (pipetting). The purified amastigotes were then assayed directly with the
115 studied compounds to check the activity upon free amastigote forms (FA), or used to
116 infect primary cultures of peritoneal macrophages (PMM) to investigate their potency
117 against intracellular forms (IA) (Feitosa LM *et al.*, 2019). Swiss male mice (18-20 g)
118 were inoculated with 3% thioglycolate, and after 4 days, PMM collected by rinsing
119 the animals' peritoneum with RPMI 1640. Mammalian cells were seeded at 24 (3×10^5
120 cells/well) and 96-wells (5×10^4 cells/well) plates and used for *in vitro* infection and
121 host cell cytotoxicity analysis, respectively. The cultures were sustained at 37°C with
122 5% CO₂ atmosphere in RPMI 1-640 medium (pH 7.2 to 7.4) without phenol red (Gibco
123 BRL) but supplemented with 1% L-glutamine, 1% PEN-STR, 10% fetal bovine serum
124 (FBS). Assays using FA were also maintained at 32°C using the same RPMI culture
125 medium but adding 5% FBS instead of 10%.

126 *Cytotoxicity upon mammalian host cells and leishmanicidal analysis:* For cytotoxicity
127 analysis, PMM were incubated for 48h with increasing concentrations of the tested
128 compounds (up to 500 μM). Cellular viability was evaluated by AlamarBlue tests
129 (Invitrogen) following the manufacturer's instructions (Da Silva *et al.*, 2007,
130 Romanha *et al.*, 2010). The leishmanicidal activity was explored in two steps: in the
131 first set of assays, amastigotes (10^6 parasites per well in 0.2mL) purified from animal
132 lesions (free amastigotes -FA) were exposed for 48 h using a fixed concentration (10
133 μM), and then, drug activity assessed by AlamarBlue tests (Mikus J & Sterverding D,
134 2000). Then, in a second set of phenotypic screenings, the activity of the compounds
135 was further validated upon intracellular amastigotes (IA). In these assays, PMM
136 (3×10^5) were infected with amastigotes (9×10^5 amastigotes) using MOI 3:1 (Van
137 Bocxlaer *et al.*, 2019). After 48 h of compound incubation (0-20 μM), infected PMM
138 were rinsed with saline buffered with phosphate (PBS), fixed with Bouin and stained
139 with Giemsa solution for light microscopy analysis (Santos *et al.*, 2019). Then, the
140 percentage of infected host cells and the number of parasites per infected cells were
141 scored for determination of the corresponding infection index (II) that represents the
142 multiplication factor of both parameters. Only characteristic parasite nuclei and
143 kinetoplasts were counted as surviving parasites since irregular structures could mean
144 parasites undergoing death. The results were expressed as % of reduction of the
145 parasite burden and the IC_{50} and IC_{90} calculated (Santos *et al.*, 2019). All assays were
146 run in at least twice in three independent repeats.

147 *Compound database preparation:* Using the LigPrep module of the Schrödinger drug
148 design software, a database (Asinex gold) of commercially available compounds was
149 prepared by performing 2D to 3D conversion, addition of hydrogens, generation of
150 ionization states, tautomeric states, stereoisomers and ring conformations at the

151 physiological pH 7.0 ± 2.0 . Further, energy minimization of all the compounds was
152 carried out using the molecular mechanics OPLS3 force field.

153 **Results**

154 *Shape-based virtual screening:* Compound GNF5343, an Oxazolo[4,5-b]pyridine
155 derivative (Figure 1) was reported to display activity against *Leishmania donovani*,
156 *Trypanosoma cruzi* and *Trypanosoma brucei* (Khare *et al.*, 2016). This compound
157 was used as a query compound to perform the virtual screening of a set of 60,000
158 chemically diverse compounds from the Asinex database. These compounds were
159 selected by applying the Lipinski filter (Mol.Wt ≤ 500 ; cLogP ≤ 5 ; HBA ≤ 10 ; HBD
160 ≤ 5), removing the compounds with nitro groups and reactive functional groups
161 (QikProp, Schrödinger release 2017-2). Using the shape-based virtual screening
162 approach, each conformer of the molecule from the database was aligned to the query
163 compound and phase sim score was computed based on the maximum overlapping
164 characteristics. Compounds with shape sim score between 0.85 to 0.6 were visually
165 inspected to assess the structural diversity and synthetic accessibility. Based on these
166 criteria, a subset of 31 compounds (Chart 1) was selected and Hierarchical clustering
167 was performed, in which 2D fingerprints and atom pairs were used as metrics to
168 quantify the chemical diversity (Canvas, Schrödinger release 2017-2). A total of 11
169 clusters were identified, of which five were singletons with diverse chemical
170 structures such as Quinoxaline derivative (cluster 4), Imidazo[2,1-b]thiazole
171 derivative (cluster 6), benzoxazole derivative (cluster 9), 2-oxo-2H-chromene
172 derivative (cluster 10) and 3-imidazo[1,2-a] pyridine derivative (cluster 11). As the
173 query compound GNF5343 was not available for purchase, we have selected one of
174 its close analogue Cp1 (Figure 1) for the comparative studies along with the selected
175 set of 31 hit compounds. Cp1 differs from GNF5343 in having a thiophenyl ring

176 substitution instead of furyl ring. All 32 compounds were purchased from Asinex and
177 assayed using different protocols *in vitro*. A fixed concentration (10 μ M) was first
178 assessed on free amastigotes (FA) and findings demonstrated that two (Cp1 and Cp2)
179 out of the 32 compounds reduced (≥ 50 %) the number of live parasites. Analogues
180 of Cp2 from cluster 1 (Chart 1: 2a and 2b) displayed weak inhibition. Compounds
181 from other clusters did not show any activity. While Cp1 is a close analogue of query
182 compound, Cp2 is structurally diverse from GNF5343 in having benzimidazole
183 scaffold. Both GNF5343 and Cp2 displayed good alignment and maximum volume
184 overlap (Figure 1) indicating that these two compounds are having similar topology
185 to form similar van der Waals surface interactions at the same region. It is interesting
186 to notice the varied distribution of hydrogen bond donors (HBD), hydrogen bond
187 acceptors (HBA) and hydrophobicity between the basic scaffolds (Oxazolo[4,5-
188 b]pyridine Vs benzimidazole) of GNF5343 and Cp2. These active compounds (Cp1
189 and Cp2) and the reference drug Pentamidine (Pt) were further analyzed against FA
190 using increasing concentrations of the tested compounds and Pt. The findings showed
191 moderate leishmanicidal effect, with IC₅₀ values of 14.93 and 15.86 μ M for Cp1 and
192 Cp2 respectively, being less potent than Pt (0.71 μ M) (Table 1). In the second round
193 of assays, the compounds were further evaluated against intracellular amastigotes
194 present in the cytoplasm of PPM, which represent the gold models for *in vitro*
195 screening of leishmanicidal agents (DNDi, 2018). Our data showed that both
196 compounds were active upon IA, exhibiting IC₅₀ values of 7 and 8.50 μ M,
197 respectively, while Pt gave 1.94 μ M (Table 1). Against the IA, Cp1 and Cp2 reached
198 low IC₉₀ values (17.25 \pm 0.21 μ M and 18.54 \pm 0.96 μ M), exhibiting a leishmanicidal
199 profile since both drastically dropped the number of parasites per cells as well as the
200 percentage of infected PMM (Figure 2). Regarding the mammalian host cell toxicity,

201 we found that after 48 h of exposure, Cp1 and Cp2 were about 3-fold less toxic as
202 compared to Pt, giving IC₅₀ of 62.75±0.27 and 65.39±0.61, with selectivity indexes
203 of 6 and 9, respectively, in similar range than the reference drug (SI = 8, Table 1).
204 *In silico* assessment of drug likeness and DMPK properties is most effective way in
205 reducing time, expenses and maximize the success in drug discovery process
206 (Lombardo *et al.*, 2017). Therefore, drug likeness and DMPK properties were
207 predicted for both Cp1 and Cp2 using the QikProp module (QikProp, Schrödinger
208 release 2017-2). Recommended compliance scores are given in Table 2. The predicted
209 properties of Cp1 and Cp2 showed compliance with “Lipinski rule of five”. According
210 to “Jorgensen rule of three” any compound that meet the recommended criteria (Table
211 2) are more likely to be orally available. The predicted properties of both Cp1 and
212 Cp2 displayed compliance with “Jorgensen rule of three”. Hence these compounds
213 could show good permeability and solubility properties. Both these properties are
214 crucial for good oral bioavailability. QPPMDCK values are the prediction of MDCK
215 cell permeability (nm/s) which is a good mimic for blood brain permeation. According
216 to this, both compounds displayed good blood brain permeation. The efficiency of a
217 drug may be affected by the extent at which it binds to human plasma protein. If
218 compounds show high binding affinity to serum albumin this could lead to poor
219 efficacy. Hence it is very crucial to understand the binding characteristics of Cp1 and
220 Cp2. The predicted human serum albumin binding values (Table 2) for both Cp1 and
221 Cp2 are within the permissible range indicating a lower binding affinity to the serum
222 albumin protein.

223

224

225

226
227
228
229
230
231
232
233
234
235
236
237
238
239
240
241
242
243
244
245
246
247
248
249
250

Discussion

The entire process of drug discovery is extremely costly and takes at least one decade of pre-clinical and clinical studies: 1 out of 10,000 drug candidates succeeds in this long flowchart, and finally reaches successfully into the market (Van Norman 2016). In this context, more reliable and reproducible experimental models (*in vitro* and *in vivo*) are needed to find better translation among pre-clinical and clinical outcomes of novel antiparasitic drugs (Chatelain & Konar 2015, Katsuno 2015). Presently, our analysis was performed using primary cultures of peritoneal macrophages infected with *L. amazonensis* since professional phagocytes are the main source of host cells for those obligate intracellular parasites (Walker *et al.*, 2015). This *in vitro* standardized experimental model for CL is claimed to closely reproduce *in vivo* conditions (Stacey 2006), therefore contributing to novel drug candidate screenings for this neglected illness (Chatelain & Ioset 2011, Caridha *et al.*, 2019). Also, although in Asia and Africa continents CL is mainly caused by *L. major* and *L. tropica*; in the Americas, the disease is triggered by a higher number of species including *L. amazonensis*, justifying the present use of this parasite species (Martins 2014, de Vries *et al.*, 2015). *L. amazonensis* is a relevant species in Brazil closely related to a wide spectrum of CL pathologies, including highly severe diffuse cutaneous leishmaniasis (Lainson, 1994). These data corroborate the choice of our *in vitro* model to explore the potential effect of novel anti-CL compounds. Another interesting point to be addressed is the use of protocols that enable the identification of antiparasitic drugs that induces rapid parasite lysis (Da Silva *et al.*, 2011). This is especial characteristic as most of the CL patients live in very poor areas with difficult access to public health assistance and then, frequently display advanced pathologies, demanding a fast *killer* drug (Ruoti *et al.*, 2013, Okwor & Uzonna 2016). Aiming to

251 fulfill this demand, we established a period of 48 h of drug exposure while testing the
252 parasites and host mammalian cells, a shorter period of incubation as compared others
253 reported in the current literature for CL *in vitro* models (Van Bocklaer, 2019).

254 Our present study explored the leishmanicidal effect of Cp1 (an analogue of
255 GNF5343) and Cp2 (a benzimidazole analogue) identified using shape-based virtual
256 screening approach. Both Cp1 and Cp2 achieved quite relevant potency against
257 amastigotes, especially those lodge inside macrophages, reaching IC₅₀ values below
258 10 μM, a considerable characteristic preconized for a hit compound with anti-
259 leishmania effect (Katsuno, 2015). Remarkably, clearance on *L. amazonensis*
260 infection was found at 20 μM in the infected PMM, a relevant feature to mitigate the
261 possible occurrence of parasite drug resistance and relapses after ceasing the drug
262 administration (Cal *et al.*, 2016). The Cp1 and Cp2 were less toxic than the reference
263 drug (pentamidine) still in use for Leishmaniasis but their selectivity indexes (>10)
264 discouraged to move them for *in vivo* proof of concept. However, their chemical
265 optimization for a wider therapeutic window and promotion of potency is largely
266 desirable to continue further studies using these compounds. It is also important to
267 state that the first-line drug pentamidine – used to treat the first stage of Sleeping
268 Sickness and CL-caused by *L. guyanensis* by over seven decades – also doesn't have
269 a desirable selectiveness *in vitro* due to high toxic profile, although display an
270 outstanding potency against these parasites. Currently, we are performing structural
271 modifications of Cp2 aiming to improve its potency, selectivity and satisfactory
272 pharmacological profile, favoring future phenotypic studies in order to move its
273 derivatives forward to new *in vitro* screening and *in vivo* evaluation, aiming to
274 contribute for drug discovery process of new therapeutic approaches for cutaneous

275 leishmaniasis. These analogues will also be tested against other parasites to assess
276 their broad-spectrum antiparasitic activity.

277

278 **FINANCIAL SUPPORT**

279 The present study was supported by grants from Fundação Carlos Chagas Filho de
280 Amparo à Pesquisa do Estado do Rio de Janeiro (FAPERJ), Conselho Nacional
281 Desenvolvimento científico e Tecnológico (CNPq), Coordenação de
282 Aperfeiçoamento de Pessoal de Nível Superior (CAPES), and Fundação Oswaldo
283 Cruz, PDTIS, PAEF/CNPq/Fiocruz. MNCS is research fellows of CNPq and CNE
284 researchers.

285

286 **ACKNOWLEDGMENTS**

287 The authors thank the Fortalecimento dos Programas de Gestão Estratégica de
288 Pesquisa da Fiocruz Rede de Plataformas Fiocruz (VPPLR - 001 - Fio 14) and the
289 Programa de Excelência Acadêmica (PROEX) from CAPES.

290

291 **REFERENCES**

292 **Alvar J, Vélez ID, Bern C, Herrero M, Desjeux P, *et al.***, (2012) Leishmaniasis
293 Worldwide and Global Estimates of Its Incidence. PLoS ONE 7(5): e35671., v. 7, p.
294 1-12 doi:10.1371/journal.pone.0035671.

295 **Bailey F, Mondragon-Shem K, Haines LR, Olabi A, Alorfi A, Ruiz-Postigo JA,**
296 ***et al.***, (2019) Cutaneous leishmaniasis and co-morbid major depressive disorder: A
297 systematic review with burden estimates.

298 **Barrett MP, Boykin DW, Brun R, & Tidwell RR.** (2007). Human African
299 trypanosomiasis: pharmacological re-engagement with a neglected disease. *British*
300 *journal of pharmacology*, 152(8), 1155–1171. <https://doi.org/10.1038/sj.bjp.0707354>

301 **Bilgic-Temel A, Murrell, DF, & Uzun S** (2019). Cutaneous leishmaniasis: A
302 neglected disfiguring disease for women. *International journal of women's*
303 *dermatology*, 5(3), 158–165. <https://doi.org/10.1016/j.ijwd.2019.01.002>

304 **Canvas, Schrödinger** Release 2017-2: Maestro, Schrödinger, LLC, New York, NY,
305 2017.

306 **Caridha D, Vesely B, van Bocxlaer K, Arana B, Mowbray CE, Rafati S, Uliana**
307 **S, Reguera R, Kreishman-Deitrick M, Sciotti R, Buffet P, Croft SL** (2019) Route
308 map for the discovery and pre-clinical development of new drugs and treatments for
309 cutaneous leishmaniasis. *Int J Parasitol Drugs Drug Resist.* 2019 Dec;11:106-117. doi:
310 10.1016/j.ijpddr.2019.06.003. PMID: 31320296; PMCID: PMC6904839.

311 **Chatelain E, Ioset JR** (2011) Drug discovery and development for neglected diseases:
312 the DNDi model. *Drug Des Devel Ther* 16;5:175-81. doi: 10.2147/DDDT.S16381.
313 PMID: 21552487; PMCID: PMC3084299.

314 **Chatelain E, Konar N** (2015) Translational challenges of animal models in Chagas
315 disease drug development: a review. *Drug Des Devel Ther* 9:4807– 4823.
316 <https://doi.org/10.2147/DDDT.S90208>.

317 **Cal M, Ioset J-R, Fügi MA, Mäser P, Kaiser M.** (2016) Assessing anti-*T. cruzi*
318 candidates in vitro for sterile cidalty. *Int J Parasitol Drugs Drug Resist* 6:165–170.
319 <https://doi.org/10.1016/j.ijpddr.2016.08.003>.

320 **Croft SL, Sundar S & Fairlamb AH** (2006). Drug resistance in leishmaniasis.
321 *Clinical microbiology reviews*, 19(1), 111–126. DOI: 10.1128/CMR.19.1.111-
322 126.2006

323 **Da Silva CF, Batista MM, Mota RA, de Souza EM, Stephens CE, Som P, Boykin**
324 **DW, Soeiro Mde N** (2007) Activity of "reversed" diamidines against *Trypanosoma*
325 *cruzi* "in vitro". *Biochem Pharmacol.* 2007 Jun 15;73 (12):1939-46

326 **de Vries HJ, Reedijk SH, Schallig HD** (2015) Cutaneous leishmaniasis: recent
327 developments in diagnosis and management. *Am J Clin Dermatol.* Apr;16(2):99-109.

328 **DNDi Annual report** (2018). Making medical history. 08/03/2020
329 https://www.dndi.org/wp-content/uploads/2019/07/DNDi_2018_AnnualReport.pdf

330 **Feitosa LM, da Silva ER, Hoelz LVB, Souza DL, Come JAASS, Cardoso-Santos**
331 **C, Batista MM, Soeiro MNC, Boechat N, Pinheiro LCS** (2019) New
332 pyrazolopyrimidine derivatives as *Leishmania amazonensis* arginase inhibitors.
333 *Bioorg Med Chem.* 15;27(14):3061-3069. doi: 10.1016/j.bmc.2019.05.026.

334 **Eiras DP, Kirkman LA & Murray HW** (2015) Cutaneous Leishmaniasis: Current
335 Treatment Practices in the USA for Returning Travelers. *Curr Treat Options Infect*
336 *Dis.* Mar 1;7(1):52-62. doi: 10.1007/s40506-015-0038-4. PMID: 25788870; PMCID:
337 PMC4360962.

338 **Godinho JL, Simas-Rodrigues C, Silva R, Ürmenyi TP, de Souza W, Rodrigues**
339 **JC** (2012) Efficacy of miltefosine treatment in *Leishmania amazonensis*-infected
340 BALB/c mice. *Int J Antimicrob Agents.* 39(4):326-31. doi:
341 10.1016/j.ijantimicag.2011.11.008. Epub 2012 Jan 9.

342 **Katsuno K, Burrows JN, Duncan K, Hooft van Huijsduijnen R, Kaneko T.** (2015)
343 Hit and lead criteria in drug discovery for infectious diseases of the developing world.
344 *Nature Reviews Drug Discovery* 14:751–758.

345

346 **Khare S, Nagle AS, Biggart A, Lai YH, , Liang F, Davis LC, Barnesn, SW,**
347 **Mathison CJN, Myburgh E, Gao, MY, Gillespie, JR, Liu X, Tan, JL, Stinson M,**

348 **Rivera, IC, , Ballard J, Yeh V, Groessl T, Federe G, Koh, HXY, Venable JD,**
349 **Bursulaya, B, Shapiro M, Mishra PK, Spraggon G, Brock A, Mottram JC,**
350 **Buckner FS, Rao SPS, Wen BG, Walker JR, Tuntland T, Molteni V, Glynne RJ,**
351 **and Supek F. (2016) Proteasome inhibition for treatment of leishmaniasis, Chagas**
352 **disease and sleeping sickness. Nature. 537(7619): 229–233.**
353 **doi:10.1038/nature19339.**

354
355 **Kumar A, Zhang KYJ. (2018) Advances in the Development of Shape Similarity**
356 **Methods and Their Application in Drug Discovery. Front. Chem. 6:315. doi:**
357 **10.3389/fchem.2018.00315.**

358
359 **Lainson R, Shaw JJ, Silveira FT, de Souza AAA, Braga RR, Ishikawa EAY**
360 **(1994) The dermal leishmaniasis of Brazil, with special reference to the eco-**
361 **epidemiology of the disease in Amazonia. Mem Inst Oswaldo Cruz. 89:435–43.**

362
363 **Lombardo F, Desai PV, Arimoto R, Desino KE, Fischer H, Keefer CE, Petersson**
364 **C, Winiwarter S, and Broccatelli F. (2017) In Silico Absorption, Distribution,**
365 **Metabolism, Excretion, and Pharmacokinetics (ADME-PK): Utility and Best**
366 **Practices. An Industry Perspective from the International Consortium for Innovation**
367 **through Quality in Pharmaceutical Development. J. Med. Chem. 60, 9097-9113.**

368
369 **López L, Vélez I, Asela C, Cruz C, Alves F, Robledo S, Arana B. (2018) A phase**
370 **II study to evaluate the safety and efficacy of topical 3% amphotericin B cream**
371 **(Anfoleish) for the treatment of uncomplicated cutaneous leishmaniasis in Colombia.**

372

373 PLoS neglected tropical diseases, 12(7), e0006653.
374 <https://doi.org/10.1371/journal.pntd.0006653>

375 **Martins AL, Barreto JA, Lauris JR, Martins AC** (2014) American tegumentary
376 leishmaniasis: correlations among immunological, histopathological and clinical
377 parameters. *An Bras Dermatol.* Jan-Feb;89(1):52-8.

378 **Mikus J & Sterverding D** (2000) A simple colorimetric to screen drug cytotoxicity
379 against *Leishmania* using the dye Alamar blue. [Parasitol Int.](#) Jan;48(3):265-9.

380 **Miranda-Verastegui C, Tulliano G, Gyorkos TW, Calderon W, Rahme E, et al.**
381 (2009) First-Line Therapy for Human Cutaneous Leishmaniasis in Peru Using the
382 TLR7 Agonist Imiquimod in Combination with Pentavalent Antimony. *PLoS Negl*
383 *Trop Dis* 3(7): e491. doi:10.1371/journal.pntd.0000491

384 QikProp, virtual screening workflow, Schrödinger Release 2017-2: Maestro,
385 Schrödinger, LLC, New York, NY, 2017.

386 **Okwor I & Uzonna J** (2016) Social and Economic Burden of Human
387 Leishmaniasis. *Am J Trop Med Hyg.* 2016;94(3):489–493.

388 **Romanha AJ, Castro SL, Soeiro Mde N, Lannes-Vieira J, Ribeiro I, Talvani A,**
389 **Bourdin B, Blum B, Olivieri B, Zani C, Spadafora C, Chiari E, Chatelain E,**
390 **Chaves G, Calzada JE, Bustamante JM, Freitas-Junior LH, Romero LI, Bahia**
391 **MT, Lotrowska M, Soares M, Andrade SG, Armstrong T, Degraeve W, Andrade**
392 **Zde A** (2010) *In vitro* and *in vivo* experimental models for drug screening and
393 development for Chagas disease. *Mem Inst Oswaldo Cruz.* 105(2):233-8

394

395 **Ruoti M, Oddone R, Lampert N, Orué E, Miles MA, Alexander N, Rehman AM,**
396 **Njord R, Shu S, Brice S, Sinclair B, Krentel A.** (2013) Mucocutaneous

397 leishmaniasis: knowledge, attitudes, and practices among paraguayan communities,
398 patients, and health professionals. *J Trop Med*.

399 **Santos CC, Lionel JR, Peres RB, Batista MM, da Silva PB, de Oliveira GM, da**
400 **Silva CF, Batista D, Souza S, Andrade CH, Neves BJ, Braga RC, Patrick DA,**
401 **Bakunova SM, Tidwell RR, Soeiro M. (2018) *In Vitro, In Silico, and In***
402 ***Vivo* Analyses of Novel Aromatic Amidines against *Trypanosoma***
403 ***cruzi*. *Antimicrobial agents and chemotherapy*, 62(2), e02205-17.**
404 **doi:10.1128/AAC.02205-17**

405 **Shirzadi MR (2019) Lipsosomal amphotericin B: a review of its properties, function,**
406 **and use for treatment of cutaneous leishmaniasis. *Research and reports in tropical***
407 ***medicine*, 10, 11–18. <https://doi.org/10.2147/RRTM.S200218>**

408 **Stacey, G. (2006) Primary Cell Cultures and Immortal Cell Lines. *Encyclopedia of***
409 ***Life Sciences*.doi:10.1038/npg.els.0003960**

410 **Swinney, DC & Anthony J (2011). How were new medicines discovered? *Nat.***
411 ***Rev. Drug Discov.* 10(7), 507-519. doi: 10.1038/nrd3480.**

412 **Valencia BM, Miller D, Witzig RS, Boggild AK, Llanos-Cuentas A (2013) Novel**
413 **Low-Cost Thermotherapy for Cutaneous Leishmaniasis in Peru. *PLoS Negl***
414 ***Trop Dis* 7(5): e2196. doi:10.1371/journal.pntd.0002196**

415 **Van Bocxlaer K, Caridha D, Black C, Vesely B, Leed S, Sciotti RJ, Wijnant GJ,**
416 **Yardley V, Braillard S, Mowbray CE, Ioset JR, Croft SL (2019) Novel**
417 **benzoxaborole, nitroimidazole and aminopyrazoles with activity against experimental**
418 **cutaneous leishmaniasis. *Int J Parasitol Drugs Drug Resist.* v11:129–138.**
419 **doi:10.1016/j.ijpddr.2019.02.002**

420 **Van Norman GA** (2016) Drugs, Devices, and the FDA: Part 1: An Overview of
421 Approval Processes for Drugs. JACC.V1(3),170-179.
422 DOI:10.1016/j.jacbts.2016.03.002

423 **Walker DM, Oghumu S, Gupta G, McGwire BS, Drew ME, Satoskar AR.**
424 **Mechanisms of cellular invasion by intracellular parasites** (2014) Cell Mol Life
425 Sci. Apr;71(7):1245-63. doi: 10.1007/s00018-013-1491-1. Epub 2013 Nov 13. PMID:
426 24221133; PMCID: PMC4107162.

427 **World Health Organization** (2020) Leishmaniasis factsheet — 2015(*last update 2*
428 *Mar. 2020*) Brazil. Retrieved from <https://www.who.int/en/news-room/factsheets/detail/leishmaniasis> Mar 8, 2020th.

430

431

432

433

434

435

436

437

438

439

440

441

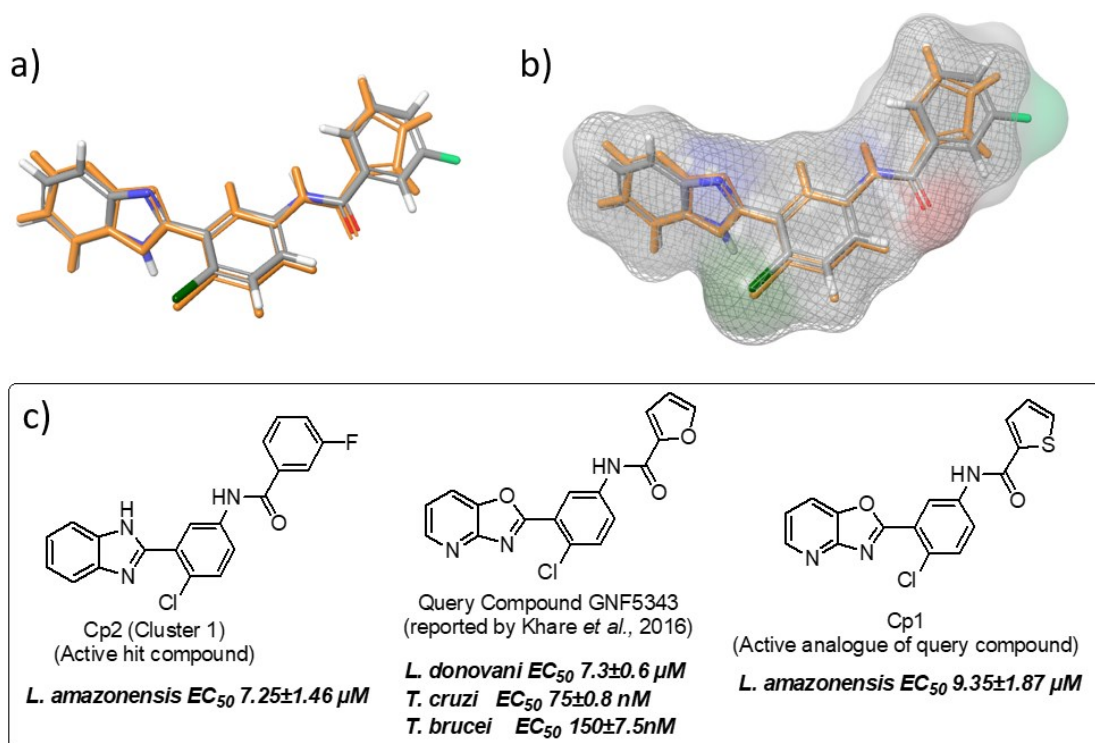
442

443

444

445

446



447

448

449

Figure 1. Shape-based virtual screening results. a) Illustrating the good alignment of

450 query compound GNF5343 (orange sticks) with compound **2** (atom type coloured sticks).

451 b) Displaying maximum volume overlap that indicates good shape complementarity

452 between the query compound (represented with mesh with an area of 300 \AA^2) and the

453 compound **2** (represented with van der Waals molecular surface area of 326.5 \AA^2).

454 c) Molecular structures and their associated activity data. 1a & 1b Images are generated

455 using Phase-Schrödinger drug design software. (Reddy, please correct “brucei” in figure

456 1c)

457

458

459

460

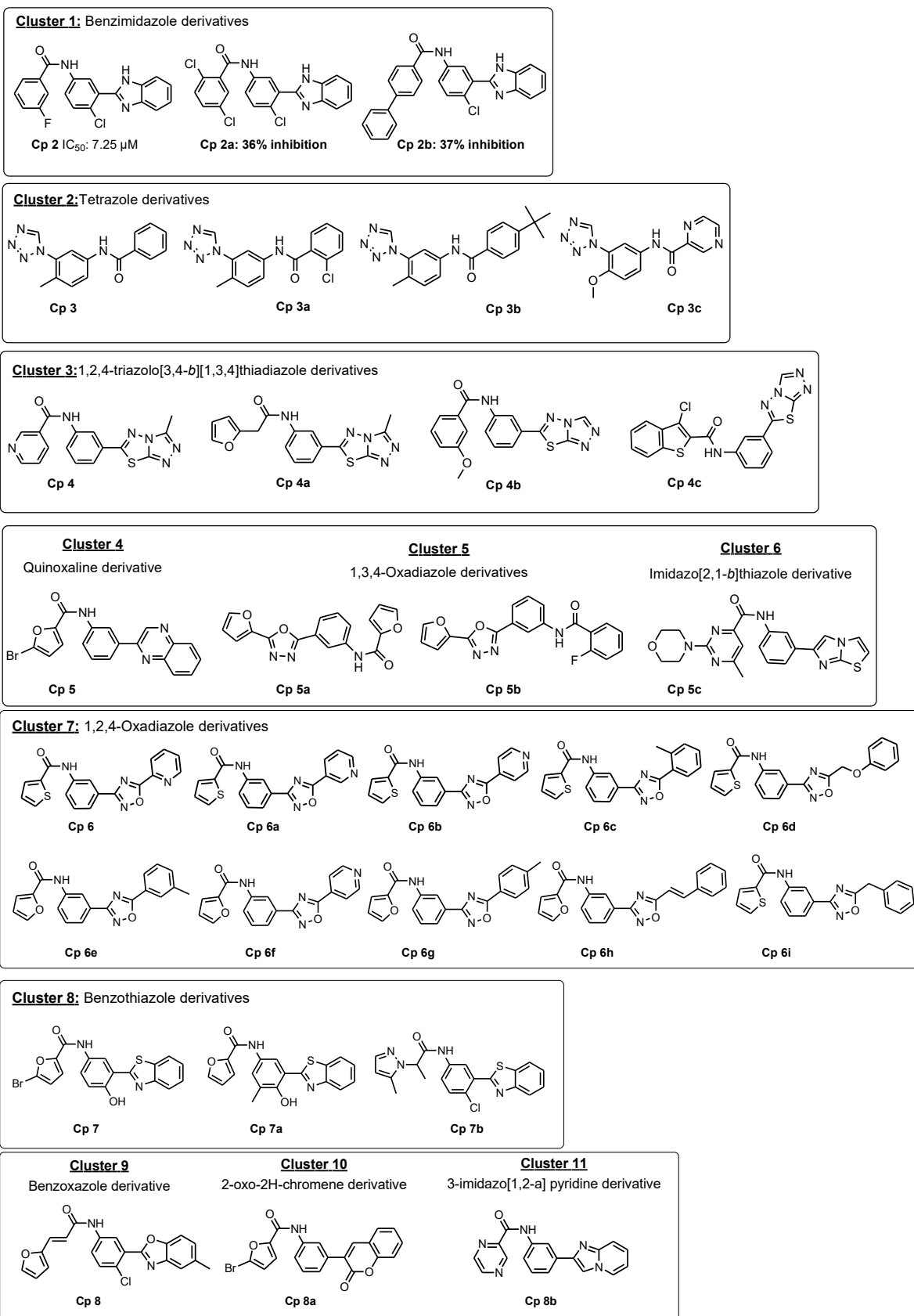
461

462

463

464
465

Chart 1. Clusters of hit compounds identified by shape-based virtual screening strategy

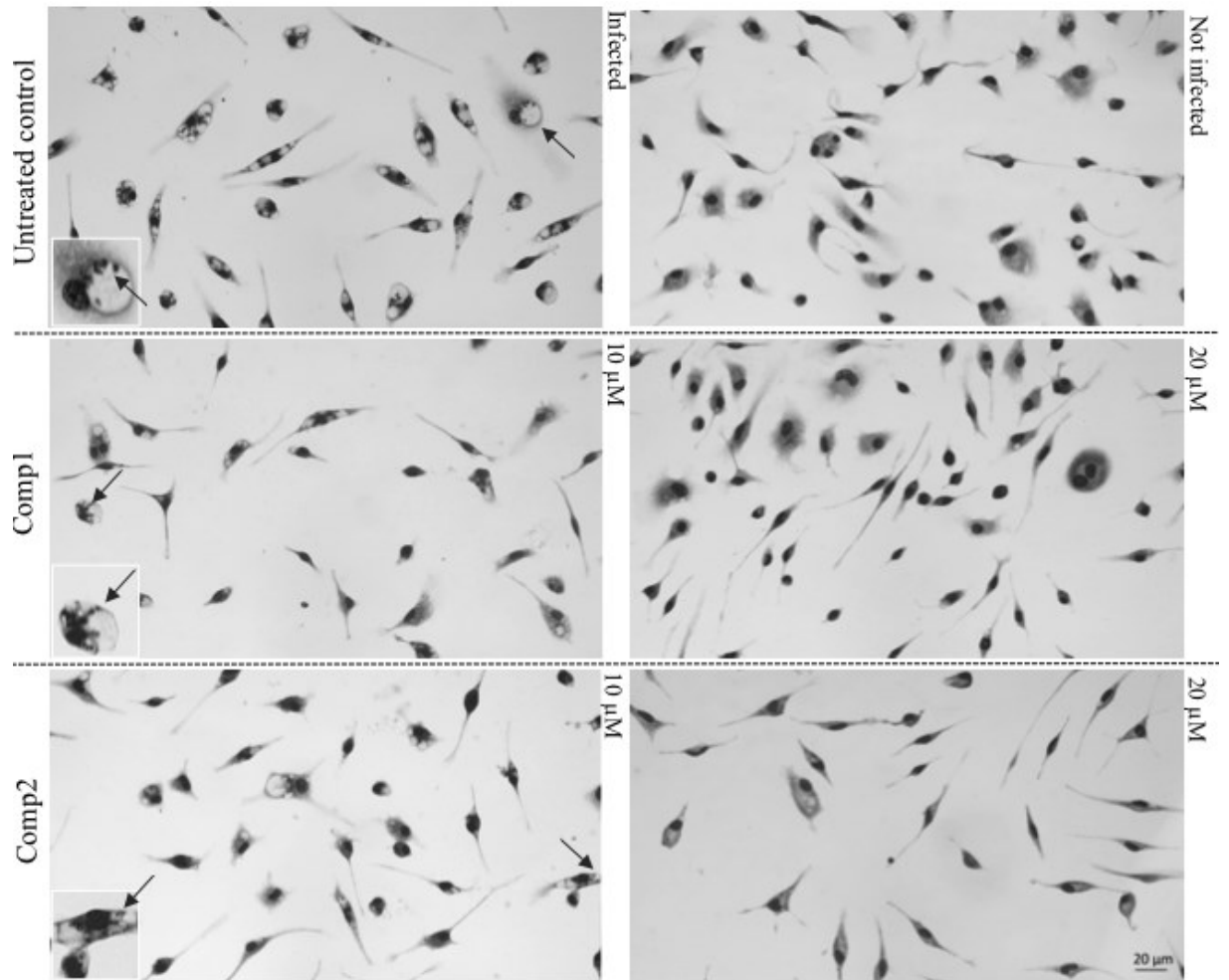


466

467

468
469

470



471

472 **Figure 2.** Light microscopy images of Giemsa-stained uninfected and infected PMM

473 submitted or not (untreated) to 10 and 20 µM of Cp1 and Cp2, demonstrating parasite

474 sterilization at 20 µM. Arrows: intracellular parasites.

475

476

477

478

479

480

481

482

483

484 **Table 1.** The leishmanicidal activity and cytotoxicity effect (IC₅₀ - mean and SD) on
 485 peritoneal macrophage (PMM) of Cp1 and Cp2. The compounds were tested (48 hours
 486 of incubation) upon amastigote forms purified from mice lesions (FA) and on
 487 intracellular amastigote forms (IA) hosted in PMM. SI: selective indexes.

488

| Compound | IC ₅₀ (μM) _{PMM} | IC ₅₀ (μM) _{FA} | IC ₅₀ (μM) _{IA} | SI _{FA} | SI _{IA} |
|-------------|--------------------------------------|-------------------------------------|-------------------------------------|------------------|------------------|
| Cp 1 | 62.75±0.27 | 13.03±2.69 | 9.35±1.87 | 4.82 | 6.71 |
| Cp 2 | 65.39±0.61 | 14.09±2.24 | 7.25±1.46 | 4.64 | 9.02 |
| Pentamidine | 15.88±0.59 | 0.71±0.05 | 1.94±0.50 | 22.37 | 8.19 |

489

490

491

492 **Table 2.** *In-silico* assessment of drug likeness and DMPK properties of Cp1 and Cp2

493

| | | Recommended compliance score (range for 95% of drugs) | Compound ID | |
|-------------------------|---------------------|---|-------------|---------|
| | | | Cp1 | Cp2 |
| Lipinski Rule of five | Mol.Wt | ≤ 500 | 355.80 | 365.794 |
| | HBD | ≤ 5 | 1 | 2 |
| | HBA | ≤ 10 | 4 | 2 |
| | cLogP | ≤5 | 3.36 | 4.59 |
| Jorgensen Rule of three | QPlogS | -6.5 to 0.5 | -5.380 | -6.289 |
| | QPCaco | <25 poor, >500 great | 1403 | 1721 |
| | Primary metabolites | <7 | 3 | 0 |
| % Human oral absorption | - | >80% is high, <25% is low | 100 | 100 |
| QPPMDCK | - | >500 great, <25 poor | 2650 | 3285 |
| QPlogKhsa | - | -1.5 to 1.5 | 0.243 | 0.616 |

494 *Mol.Wt*: Molecular Weight; *HBD*: hydrogen bond donor; *HBA*: hydrogen bond acceptor; *cLogP*:
 495 calculated logarithm of partition coefficient; *QPlogS*: the logarithm of aqueous solubility;
 496 *QPCaco*: Caco-2 cell permeability in nm/sec, model for the gut-blood barrier; *QPPMDCK*:
 497 Madin-Darby canine kidney (MDCK) cell permeability in nm/sec, model for the blood-brain
 498 barrier; *QPlogKhsa*: the logarithm of predicted binding constant to human serum albumin.

499

500